



Article

Research on Spatial Distribution Pattern of Stability Inter-Controlled Factors of Fine-Grained Sediments in Debris Flow Gullies—A Case Study

Qinjun Wang^{1,2,3,4,5,*}, Jingjing Xie^{1,2,3}, Jingyi Yang^{1,2,3}, Peng Liu^{1,2,3}, Wentao Xu^{1,2,3} and Boqi Yuan^{1,2,3}

- ¹ International Research Center of Big Data for Sustainable Development Goals, Beijing 100094, China; xiejingjing19@mails.ucas.ac.cn (J.X.); yangjingyi211@mails.ucas.ac.cn (J.Y.); liup@aircas.ac.cn (P.L.); 07182642@cumt.edu.cn (W.X.); yuanboqi23@mails.ucas.ac.cn (B.Y.)
 - ² Key Laboratory of Digital Earth Science, Aerospace Information Research Institute, Chinese Academy of Sciences, Beijing 100094, China
 - ³ University of Chinese Academy of Sciences, Yanqi Lake Campus of Chinese Academy of Sciences University, Beijing 101408, China
 - ⁴ Key Laboratory of the Earth Observation of Hainan Province, Hainan Aerospace Information Research Institute, Sanya 572029, China
 - ⁵ Kashgar Zhongke Aerospace Information Research Institute, Kashgar 844199, China
- * Correspondence: wangqj@radi.ac.cn

Abstract: Studies on the stability inter-controlled factors of fine-grained sediments in debris flow gullies play an important role in predicting the scale and danger of debris flows. However, up to the present, few studies have been carried out on the spatial distribution pattern and causes of stability inter-controlled factors of fine-grained sediments in debris flow gullies, leading to difficulty in finding the dangerous section of debris flow gullies to be monitored and controlled to reduce disaster losses. Therefore, the objective of this paper is to analyze the spatial distribution pattern and causes of stability inter-controlled factors (grain size, permeability coefficient, shear strength, and porosity), taking the Beichuan Debris Flow Gully, China, as a case. After collecting soil samples in the field, we carried out experiments to measure the stability inter-controlled factors and, from these, the results show that (1) fine-grained sediments in this case are mainly silty loams, which are stable under non-heavy rains; (2) the grain size of silty loams is mainly concentrated between 10 and 20 μm , with a spatial distribution pattern of fine in the middle and coarse at both ends; (3) the permeability coefficient of silty loams is concentrated between 1.15 and 2.17 m/d, with a spatial distribution pattern of high in the middle and low at both ends; (4) the average cohesion of silty loams is mainly concentrated between 20 and 30 kPa, with a spatial distribution pattern of low in the middle and high at both ends; and (5) the internal friction angle of silty loams is concentrated between 18.98 and 21.8°, with a spatial distribution pattern of high in the middle and low at both ends. The main reasons for these spatial distribution patterns are analyzed from three aspects of shear strength, water flow velocity, and terrain, which can provide a scientific basis for the prediction of debris flow disasters in such areas.

Keywords: debris flow gully; fine-grained sediments; soil stability; inter-controlled factors; Beichuan; particle size



Citation: Wang, Q.; Xie, J.; Yang, J.; Liu, P.; Xu, W.; Yuan, B. Research on Spatial Distribution Pattern of Stability Inter-Controlled Factors of Fine-Grained Sediments in Debris Flow Gullies—A Case Study. *Water* **2024**, *16*, 634. <https://doi.org/10.3390/w16050634>

Academic Editors: Qingzhao Zhang and Danyi Shen

Received: 18 January 2024

Revised: 14 February 2024

Accepted: 16 February 2024

Published: 21 February 2024



Copyright: © 2024 by the authors. Licensee MDPI, Basel, Switzerland. This article is an open access article distributed under the terms and conditions of the Creative Commons Attribution (CC BY) license (<https://creativecommons.org/licenses/by/4.0/>).

1. Introduction

In recent years, due to the comprehensive impacts of tectonic activities and climate change, the frequency and scale of debris flow disasters have increased, causing serious impacts on people's lives and property, and have attracted a lot of attention from countries and scholars to carry out research.

The effects of slope on water flow, the influence of material composition and grain size distribution on the initiation conditions of debris flows [1–5], and the disaster mechanisms were studied from the aspects of material source characteristics [6–8], rainfall conditions [9–12], terrain and geomorphic conditions [13], tectonic activities [14], etc. Based on these, debris flow initiation models were established, such as mathematical modeling [15] and hydrodynamic models [16–18].

Debris-flow-influencing factors and their relationships with the outflow, disaster chains, and principles of lateral erosion were studied, such as relationships between maximum runout amount and risk-assessment-influencing factors [19–22]. Based on these, models for danger sensing and prediction for debris flows were established, such as critical rainfall patterns [23], gully formation types [24], and hazard assessment and prevention models [25–29].

Based on three disaster modes (channel blocked, channel undercut, and landslide recharged), plans for disaster prevention and control were proposed, such as sediment mitigation measures [30], and hazard source analysis and prevention were based on hazard assessment and formation mechanism analysis [31–36].

As we know, during the initiation, transportation, and aggregation of debris flow, fine-grained sediments (quaternary sediments with a grain size of less than 2 mm) in debris flow gullies play a starring role, increasing the density, amplifying the danger of debris flows, and thus increasing the difficulty of debris flow prevention and control. Therefore, strengthening the research on stability inter-controlled factors of fine-grained sediments in debris flow gullies plays an important role in predicting the scale and danger of debris flows.

The stability inter-controlled factors of fine-grained sediments mainly include grain size, permeability coefficient, shear strength, and porosity. Grain size refers to the particle diameter of sediments; the permeability coefficient is the unit flow rate under a unit hydraulic gradient; shear strength refers to the ultimate strength of soil to resist shear failure, which includes cohesion and effective internal friction angle; and porosity is the percentage of soil pores per unit volume.

There are some studies on fine-grained sediments in debris flow gullies: (1) erosion characteristics [37], hydrodynamic conditions [38], and grain size distribution characteristics of sediments were studied [39], and (2) the relationship between permeability coefficient and its influencing factors [40], as well as that between cohesion and its influencing factors, was analyzed [41]. Based on these, hyperspectral detection models for cohesion [42] and permeability coefficient were also established [43], and (3) the permeability characteristics and transport principles of channel sediments were summarized, and a start-up model for loose sediments was established [44].

However, up to the present, there is no research on the spatial distribution pattern and causes of the stability inter-controlled factors of fine-grained sediments in debris flow gullies, resulting in difficulty in locating dangerous river sections for prevention. Therefore, the objective of this paper is to analyze the spatial distribution pattern and causes of the stability inter-controlled factors. According to this, we can find unstable river sections for debris flow disaster prevention.

2. Study Area

As shown in Figure 1, the study area is located in Laobeichuan County, Sichuan Province, China, with geographic coordinates of 104°14′–104°33.5′ E, 31°47.9′–31°53.5′ N, covering an area of 341 km². It belongs to a subtropical humid monsoon climate zone, with an annual average temperature of 15.6 °C and an annual average rainfall of 1399.1 mm. Of this, 70% of the annual rainfall is concentrated from June to September [11,34]. The strata of the study area mainly include the Dengying strata from the Upper Sinian, the Qingping strata from the Lower Cambrian, the Maoxian Group from the Upper and Middle Silurian, and the Quaternary sediments. In these, the main rock types include dark gray

siltstone, siliceous rock, phosphorous mudstone, phosphorous limestone, phyllite, slate, schist, limestone, sand shale, and sandy soils [13].

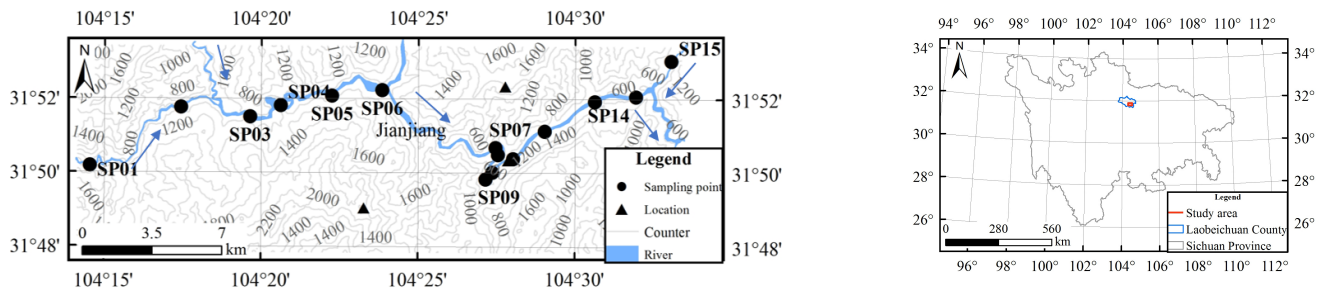


Figure 1. Map of the study area (left), the blue arrow indicates the direction of water flow) with location in Sichuan Province (right).

The main lithology in the study area indicates that most of the metamorphic rocks, marls, and Quaternary sediments have poor stability and could easily form debris flows. Especially, the Wenchuan earthquake with MS8.0 magnitude on 12 May 2008 caused severe strata fragmentation, resulting in a large number of loose sediment events like landslides, landslips, etc. Under the triggering of heavy rainfall, multiple serious debris flow disasters occurred on 20 August 2019, 11 July 2018, 28 July 2016, etc. They not only destroyed farmlands, roads, and bridges but also broke power and communication facilities, causing significant economic losses and posing a serious threat to the residential settlements [28].

3. Data and Equipment

As shown in Table 1, the Gaofen-2 (GF-2) remote sensing image covering the study area is first acquired with the highest spatial resolution of 0.8 m. Using this, the locations of fine-grained sediments in the debris flow gully are extracted (SP01–SP15 sampling points in Figure 1). Then, the DEM data are acquired to analyze elevation of the study area. Finally, after the debris flow disaster on 20 August 2019, 200 soil samples were obtained from 15 sampling points using a ring cutter between 19 and 25 March 2021 and the number of samples at each sampling points is shown in Table 2. Each sample has a volume of 600 mL and a weight of about 1 kg. With a diameter of 7 cm and a depth of 5.2 cm, the volume of the ring knife is 200 mL. Using this, the sampling procedure for a soil sample is as follows: ① clean the ring knife using a soft cloth; ② put it into the sediment vertically. When it is full of soil, pull it out and cut off the over-flowing soil with a knife. Thus, a soil sample with a volume of 200 mL is collected; ③ put the soil sample into a plastic bag and seal it immediately. After collecting three soil samples in the same plastic bag according to the above steps, seal the plastic bag and consider it as a sample with a volume of 600 mL and put it into a cotton bag; ④ record the sample number and its geographical location using a global positioning system (GPS) and write the sample number on the cloth sample bag with a marker [43].

Table 1. Data and equipment table.

| Materials | Equipment | Manufacturer/Provider |
|-------------------------------|--|--|
| Remote sensing images | Gaofen-2 (GF-2) | Land satellite remote sensing application center, Beijing, China |
| Digital elevation model (DEM) | Advanced Spaceborne Thermal Emission and Reflection Radiometer (ASTER) | Ministry of International Trade and Industry, Tokyo, Japan |
| Soil | Ring knife (200 mL) | Longnian Hardware Tools Store, Suqian, China |
| Particle size | Mhcrotra-S3500 | Microtrac MR B, Montgomeryville, PA, USA |

Table 1. *Cont.*

| Materials | Equipment | Manufacturer/Provider |
|--------------------------|--|--|
| Permeability coefficient | TST-55 permeameter | Zhejiang Dadi Instrument Co., Ltd., Shaoxing, Zhejiang, China |
| Density | MDJ-300A solid densitometer | Shanghai Lichen Instrument Technology Co., Ltd., Shanghai, China |
| Porosity | TST-55 permeameter | Zhejiang Dadi Instrument Co., Ltd., Shaoxing, Zhejiang, China |
| Shear strength | ZJ strain-controlled direct shear instrument | Nanjing soil instrument factory Company Limited (Co., Ltd.), Nanjing, Jiangsu, China |

Table 2. Number of samples at each sampling points.

| Sampling Points | Number | Sampling Points | Number |
|-----------------|--------|-----------------|--------|
| SP01 | 20 | SP09 | 20 |
| SP02 | 15 | SP10 | 10 |
| SP03 | 15 | SP11 | 10 |
| SP04 | 15 | SP12 | 10 |
| SP05 | 20 | SP13 | 10 |
| SP06 | 15 | SP14 | 10 |
| SP07 | 10 | SP15 | 10 |
| SP08 | 10 | | |
| Total | | | 200 |

Based on these steps, experiments are carried out to measure density, grain size, permeability coefficient, and shear strength of samples.

4. Methodology

The flow chart for studying stability inter-controlled factors of fine-grained sediments is shown in Figure 2. On the basis of obtaining remote sensing, DEM, and geological background data of the study area, experiments are carried out to measure the stability inter-controlled factors, such as grain size, permeability coefficient, shear strength, and porosity. Based on these, the spatial distribution patterns of stability inter-controlled factors of fine-grained sediments are summarized, and the risk of debris flow disasters is analyzed to provide a scientific basis for the prevention and control of geological disasters in the study area.

4.1. Grain Size Measurement

Grain size refers to the particle diameter, which has some impacts on the porosity and permeability coefficient of fine-grained sediments, thereby controlling the sediment stability. We use the Microtrac S3500 laser analyzer to measure the grain size of the sediments whose main steps and results can be found in [43]. The results indicate that the grain size of fine-grained sediments in the study area is mainly concentrated between 10 and 20 μm , belonging to the silty loams [45]. The average grain size of each sampling point is shown in Figure 3, showing a spatial distribution pattern of fine in the middle and coarse at both ends.

4.2. Permeability Coefficient Measurement

The permeability coefficient, also known as the hydraulic conductivity coefficient, is the unit flow rate under a unit hydraulic gradient. It mainly reflects the size, number, and connectivity of soil pores [46], and is the main parameter controlling the stability of fine-grained sediments. The permeability coefficient of fine-grained sediments in the study area is measured using a TST-55 permeability meter, whose process and results are shown in [40]. The permeability coefficients of most fine-grained sediments in the study area are concentrated between 1.15 and 2.17 m/d, which can be classified as medium permeability

and stable in the case of non-heavy rains. The average permeability coefficient of each sampling point is shown in Figure 4, showing a spatial distribution pattern of high in the middle and low at both ends.

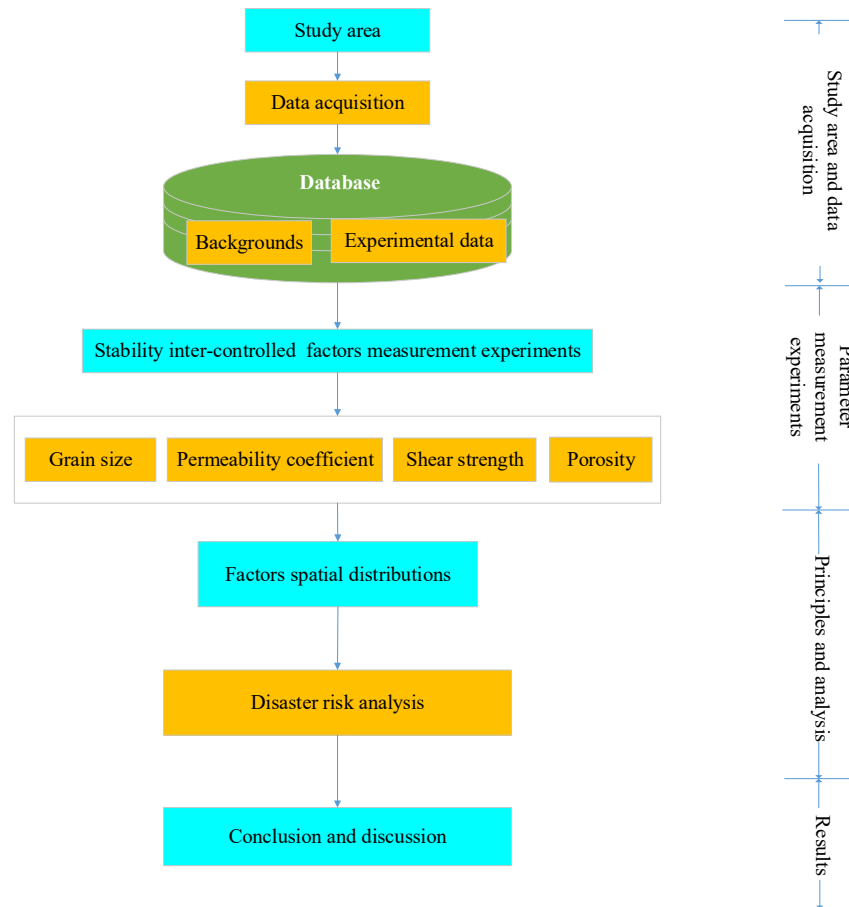


Figure 2. Flow chart for studying the spatial distribution pattern of stability inter-controlled factors of fine-grained sediments in debris flow gullies.

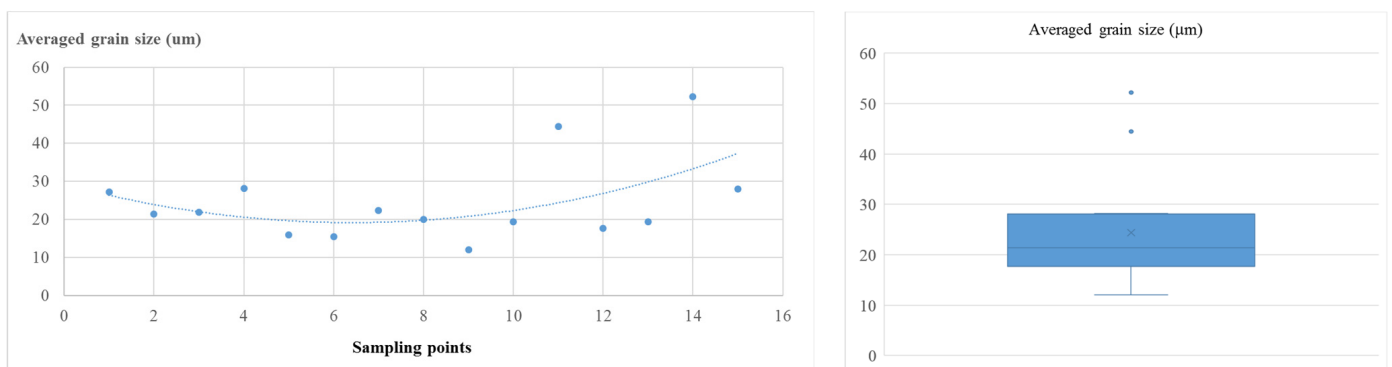


Figure 3. Average grain size distribution pattern of fine-grained sediments (left) and its box-whisker plot (right).

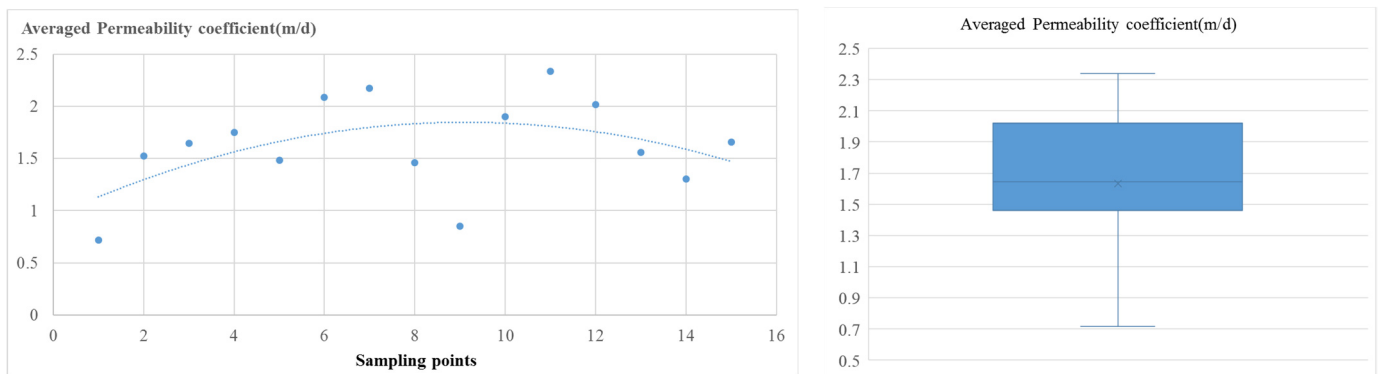


Figure 4. Distribution pattern of the average permeability coefficient of fine-grained sediments (**left**) and its box-whisker plot (**right**).

4.3. Shear Strength Measurement

Including cohesion and effective internal friction angle, shear strength refers to the ultimate strength of soil to resist shear failure, which is an important parameter to measure stability of fine-grained sediments. Cohesion is the mutual attraction between adjacent parts within the same substance; the effective internal friction angle indicates the magnitude of internal friction between soil particles, including the surface friction forces and the biting forces generated by the embedding and interlocking between soil particles. To measure the cohesion and effective internal friction angle of fine-grained sediments in the study area, a ZJ strain-controlled direct shear instrument is used, whose steps and results are shown in [43]. As shown in Figure 5, the average cohesion is mainly concentrated between 20 and 30 kPa with a spatial distribution pattern of low in the middle and high at both ends. On the other hand, as shown in Figure 6, the internal friction angle is concentrated between 18.98° and 21.8° with a spatial distribution pattern of high in the middle and low at both ends.

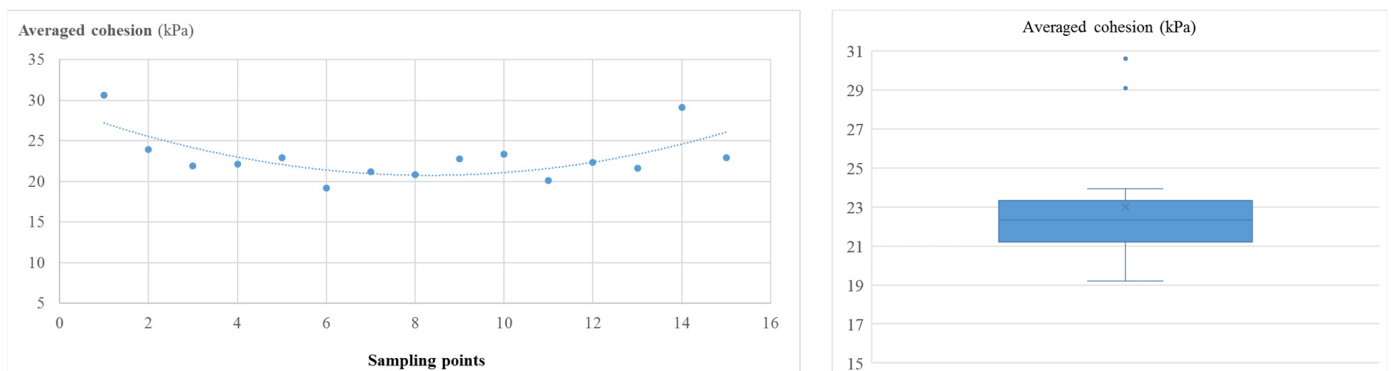


Figure 5. Spatial distribution pattern of averaged cohesion of fine-grained sediments (**left**) and its box-whisker plot (**right**).

4.4. Porosity Measurement

Porosity is the percentage of soil pores per unit volume, which is the space for water movement and storage, and the key factor influencing soil permeability and thus determining surface runoff rate. The steps and results of measuring porosity using a TST-55 permeameter can be found in [43]. The porosity of fine-grained sediments in the study area is mainly concentrated between 52 and 68%, belonging to the medium to high porosity. The average porosity of each sampling point is shown in Figure 7. The average porosity is relatively high at SP09.

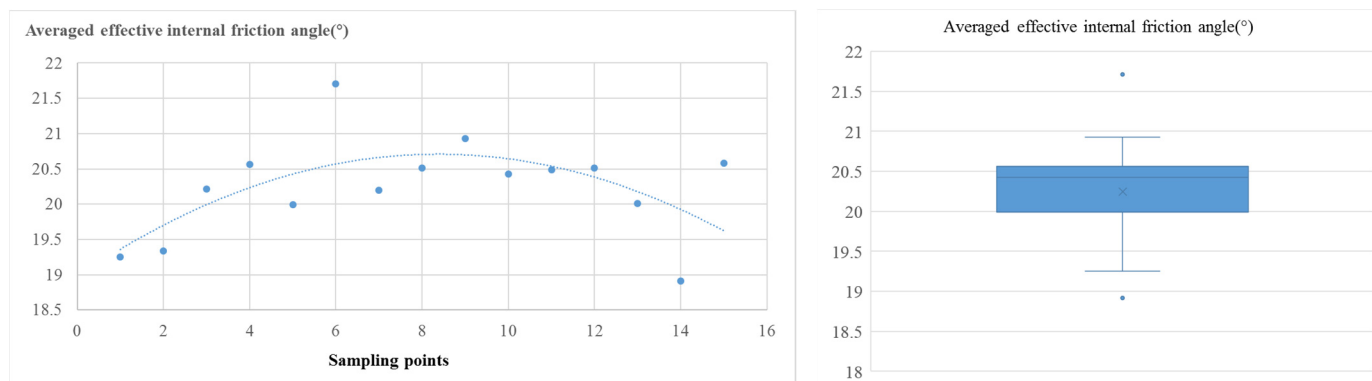


Figure 6. Spatial distribution pattern of averaged internal friction angle of fine-grained sediments (left) and its box-whisker plot (right).

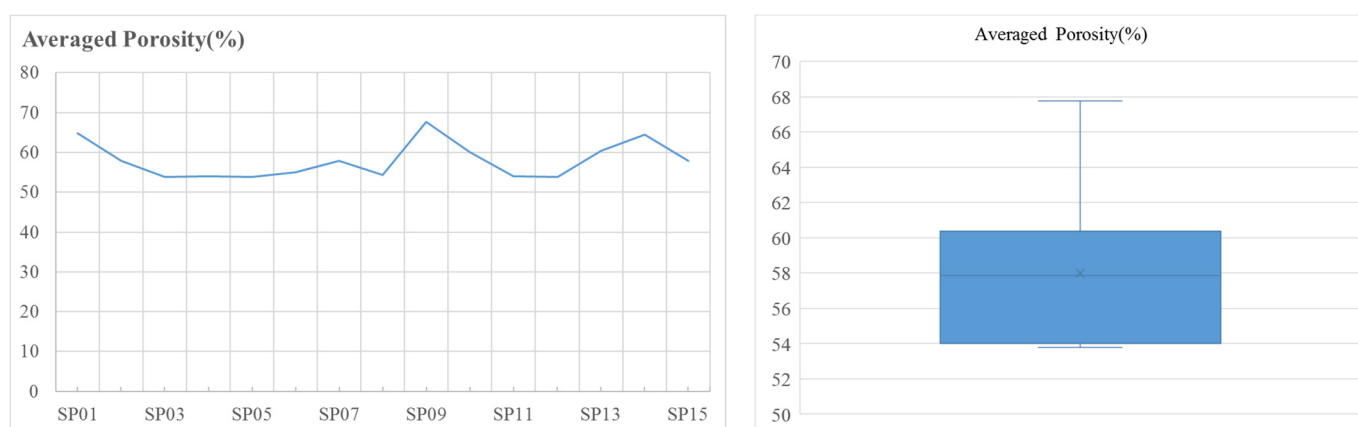
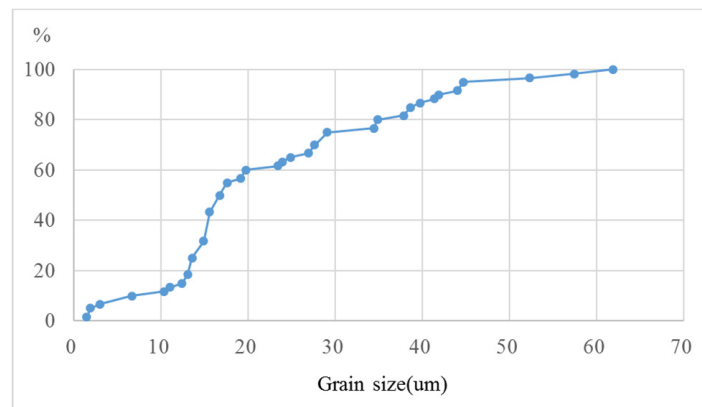


Figure 7. Spatial distribution pattern of averaged porosity of fine-grained sediments (left) and its box-whisker plot (right).

5. Results

Based on the variation characteristics of grain size, permeability coefficient, cohesion, and internal friction angle of fine-grained sediments along the Jianjiang River (Figures 3–7), the sampling points are divided into three sections: upstream (SP01–SP05), midstream (SP06–SP12), and downstream (SP13–SP15). Their characteristics are summarized as follows.

In the upstream (SP01–SP05), (1) the fine-grained sediments are mainly composed of silty loams, with an average grain size of 22.94 μm , and a downward trend from SP01 to SP05; (2) the average permeability coefficient is 1.42 m/d, belonging to medium permeability and showing an upward trend from SP01 to SP05; (3) the average cohesion is 24.3 kPa, showing a decreasing trend from SP01 to SP05 (Figure 5), and the average internal friction angle is 19.87°, showing an upward trend from SP01 to SP05 (Figure 6); (4) the cumulative distribution pattern of grain size (Figure 8) shows inflection points at 10, 20, and 30 μm , indicating poor sorting characteristics. On-site photos (SP01–SP05, Figure 8) also confirm the above conclusion: soils at SP01 are in a plate condensed state with the characteristics of high cohesion and strong erosion resistance. However, the following photos of SP02–SP05 show that the sediments are loosely accumulated, indicating low cohesion and high permeability. Therefore, for SP01 to SP05, we draw a conclusion that the soil's ability to resist water flow erosion becomes strong to weak, resulting in the risk of debris flow disasters becoming weak to strong.



Grain size cumulative distribution curve of SP01–SP05



Photo of SP01 (No. 567)



Photo of SP02 (No. 563)



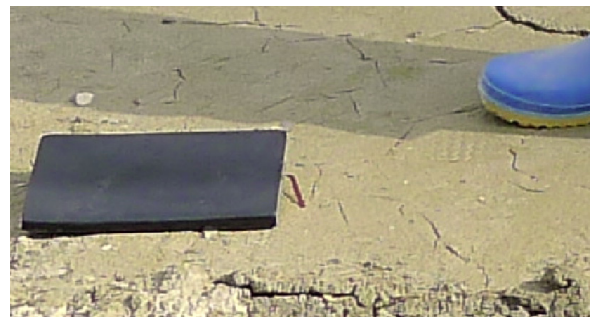
Photo of SP03 (No. 560)



Photo of SP04 (No. 557)



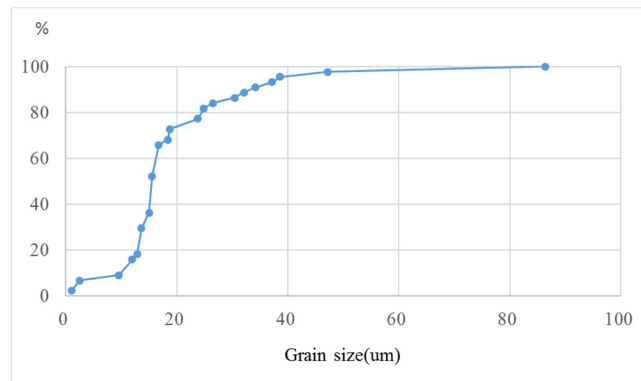
Photo of SP05 (No. 553)



Zoomed-in image of SP01 (No. 567)

Figure 8. Cumulative grain size distribution curve and field photos of fine-grained sediments in upstream river (SP01–SP05).

In the midstream (SP06–SP12), the fine-grained sediments are mainly composed of silty loams. (1) The average grain size of the sediments in this section is 17.83 μm . Except for the coarse grain size at SP11, grain sizes at other points are almost the same and distributed horizontally (Figure 3). The cumulative distribution curve indicates the distribution of grain size in this section concentrates between 10 and 40 μm with good sorting; (2) the average permeability coefficient of the sediments in this section is 1.83 m/d, belonging to medium permeability (Figure 4); (3) the average cohesion of the sediments in this section is 21.4 kPa with an averaged internal friction angle of 20.68°. Except for the high internal friction angle at SP06, internal friction angles at other points are horizontally distributed (Figure 6). On-site photos (SP06–SP12, Figure 9) also confirm the above conclusion: the silty loams in this section are in a loose accumulation state with fine grain size, high moisture content, good sorting, and relatively poor erosion resistance, leading to increased instability of the sediments and the high risk of debris flow disasters.



Grain size cumulative distribution curve of SP06–SP12



Photo of SP06 (No. 549)



Photo of SP07 (No. 545)



Photo of SP08 (No. 541)



Photo of SP09 (No. 571)

Figure 9. Cont.



Photo of SP10 (No. 536)



Photo of SP11 (No. 516)



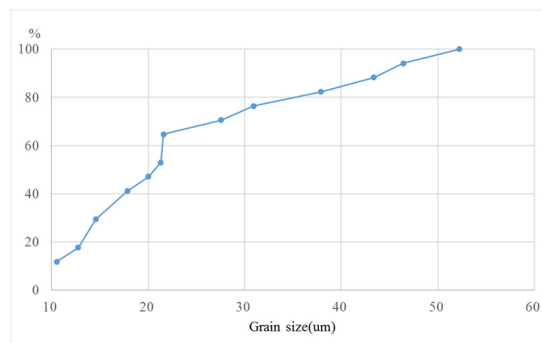
Photo of SP12 (No. 518)



Zoomed-in image of SP08 (No. 541)

Figure 9. Cumulative grain size distribution curve and field photos of fine-grained sediments in midstream river (SP06–SP12).

In the downstream (SP13–SP15), the fine-grained sediments are mainly composed of silty loams, with an average grain size of $33.23 \mu\text{m}$. (1) Compared to the sediments in the upstream and midstream, their grain size is coarser and gradually increases from SP13 to SP15 (Figure 3). The cumulative distribution curve of grain size in the downstream shows that, except for a sharp increase at $22 \mu\text{m}$, the grain size of the sediments is concentrated from 10 to $52 \mu\text{m}$, indicating the general sorting characteristics (Figure 10); (2) the average permeability coefficient of the sediments is 1.51 m/d , belonging to medium permeability, showing a gradually decreasing trend from SP13 to SP15 (Figure 4); (3) the average cohesion of the sediments is 24.53 kPa , showing an upward trend from SP13 to SP15 (Figure 5), and the average internal friction angle is 19.83° and, except for the high internal friction angle at SP15, it shows a decreasing trend (Figure 6). The on-site photos (SP13–SP15, Figure 10) also confirm the above conclusion: the silty loams in this section are in a loose accumulation state with low water content, coarse sand particles filled with clays, average sorting, and relatively strong erosion resistance, which increases the sediment stability and thus reduces the risk of debris flow disasters.



Grain size cumulative distribution curve of SP13–SP15



Photo of SP13 (No. 522)



Photo of SP14 (No. 527)



Photo of SP15 (No. 531)



Zoomed-in image of SP15 (No. 531)

Figure 10. Cumulative grain size distribution curve and field photos of fine-grained sediments in downstream river (SP13–SP15).

6. Discussion

Reasons for the results are discussed as follows.

In the upstream (SP01–SP05), compared to midstream (SP06–SP12), this section has the characteristics of low permeability coefficient, low effective internal friction angle, and high cohesion. Reasons for this phenomenon are mainly because it is located in the upstream river and easily eroded due to the water flow, tributary effect, elevation difference between this section and its surroundings, etc. The relatively fine-grained sediments are carried to the middle and downstream of the river, thus depositing relatively coarse-grained sediments. Clay minerals can easily fill in the large pores between coarse particles, resulting in relatively poor sorting of the sediments in this section with low permeability coefficient, low effective internal friction angle, and high cohesion. From these, we can see that the risk of debris flow disasters becomes weak to strong from SP01 to SP05 and the outbreak of debris flow is the result of the comprehensive effects of sediment seepage field and stress field: ① the permeability coefficient is the main parameter of the sediment seepage field. The seepage field is not only a storage environment but also a component of sediments.

Sediments with high permeability coefficients are prone to let water infiltrate to the bottom, increasing their own gravity and forming pore water pressure to break the sediment stability, thereby increasing the probability of debris flow disasters. The permeability coefficient shows an upward trend from SP01 to SP05 and the risk of debris flow disasters becomes weak to strong from SP01 to SP05. ② Shear strength is the main parameter of sediment stress field. When the shear stress meets the maximum shear strength of the sediments, they collapse and then slide with the water flow, resulting in debris flow disasters. Sediments with high shear strength have strong cohesion, high stability, and are less prone to erosion, thus providing fewer material sources for debris flow disasters. On the contrary, sediments with low shear strength can provide more material sources, resulting in a larger scale and more dangerous debris flow disaster. Cohesion shows a decreasing trend from SP01 to SP05, and the risk of debris flow disasters becomes weak to strong.

In the midstream (SP06–SP12), compared to upstream and downstream, sediments in this section have the characteristics of high permeability coefficient, high effective internal friction angle, and low cohesion. The main reason for this phenomenon is that the terrain of this section is relatively low and the river channels are winding with high curvature: the low river terrain in the high surrounding mountain terrain results in the accumulation of water during the rainy season, leading to a large water supply and causing severe soil erosion. Based on this, the high-density debris flow forms from west to east. At the same time, this section is also blocked by its high curvature, especially the highest curvature from SP07 to SP09, resulting in a severe decrease in water flow velocity, which weakens the river's sand-carrying capacity and makes it easily form good sorting sediments. Therefore, compared to the sediments in the upstream and downstream, the silty loams in this section have the characteristics of finer grain size and better sorting with high permeability coefficient, high effective internal friction angle, and low cohesion, and thus leading to high instability of sediments. So, the risk of debris flow disasters in this section is relatively high and thus needs more attention to monitor and control it, especially from SP07 to SP09 with the highest curvature.

In the downstream (SP13–SP15), compared to the sediments in the midstream, the sediments in this section show the characteristics of coarse grain size, low permeability coefficient, low effective internal friction angle, and high cohesion. The main reason for this phenomenon is mainly that there is a significant elevation difference between this section and its surroundings, resulting in high water flow speed with strong sediment-transporting capacity. Fine-grained sediments are transported far, while the coarse-grained sediments are left here, which are prone to adsorb clay particles, and thus resulting in low permeability coefficient, low effective internal friction angle, and high cohesion. According to poor conditions of low permeability coefficient and high cohesion, the risk of debris flow disasters happening in this section is relatively low.

As to the spatial distribution pattern of the stability inter-controlled factors of fine-grained sediments in the whole debris flow gully, we can discuss it as follows.

The average grain size of fine-grained sediments in the study area is relatively coarse with poor sorting in the upstream and downstream river, while it is relatively fine with good sorting in the midstream. The reason for this phenomenon is that the finer the grain size of sediments is, the farther they can be transported. Therefore, in general, rivers always show a characteristic of coarse to fine grain size from upstream to downstream. However, in this study area, due to the impact of high curvature in the middle stream, the water flow velocity slows down, which decreases the sand-carrying capacity, thus forming a sedimentary environment to make the sediments deposit with the characteristics of fine grain, good sorting, and high permeability coefficient.

The average permeability coefficient is relatively low in the upstream and downstream river and high in the middle. This is mainly related to the sediment properties: the grain size of the upstream and downstream sediments is heterogeneous and fine-grained particles are easily adsorbed among coarse-grained ones, resulting in pore blockage and thereby reducing their permeability coefficients. Meanwhile, the grain size of the sediments in the

midstream river is relatively uniform, with good sorting and independent space between particles, thus leading to relatively large porosity and good permeability coefficient.

At 22.99 kPa, the average cohesion of the whole gully has a medium to low level with poor stability [47], which is relatively high in the upstream and downstream and low in the midstream. Therefore, it is prone to erosion and transportation, resulting in the formation of debris flows and thus needing to be monitored and controlled with more attention in the midstream river.

Based on sedimentology, the main reasons for the spatial distribution of the stability inter-controlled factors of fine-grained sediments in debris flow gullies are discussed as follows.

The first reason is shear strength. Sediments with high shear strength have strong cohesion, are not easily eroded, and thus have a high stability and a short transporting distance in rivers, making them form coarse-grained sediments with poor sorting. On the contrary, sediments with low shear strength have lower stability and longer transporting distances in rivers, making them easily form fine-grained sediments with good sorting.

The second reason is water flow velocity. The water flow velocity determines the erosion and transporting capacity of a river. Under the same conditions, the faster the velocity of the water flow is, the higher the erosion ability and the stronger the carrying capacity of the rivers. The grain size of sediments is relatively coarse, with poor sorting and low permeability coefficient. On the contrary, the slower the water flow velocity is, the weaker the transporting capacity of the river becomes, and the easier it is to form a sedimentary environment. The grain size of sediments becomes finer and the permeability coefficient becomes higher. This also explains why the sediments from SP07–SP09 show finer grain size with higher permeability coefficient: due to the high curvature of the river in this section, the water flow velocity slows down. Sediments transported from upstream are prone to deposit, leading to the formation of fine-grained sediments with good sorting and high permeability coefficient.

The third reason is terrain. As we know, terrain controls potential energy and water flow velocity, thereby controlling the degree and scope of sediment erosion and thus controlling the danger of debris flow disasters. Under the same rainfall, the steeper the terrain is, the faster the water flow on the surrounding slopes becomes, thus resulting in stronger erosion ability, which generates more sources of sediments with longer transporting distances. On the contrary, the gentler the terrain is, the fewer material sources are generated and the shorter the sediments' transport. Therefore, terrain also controls the spatial distribution pattern of the sediments.

7. Conclusions

In this study, the spatial distribution patterns of stability inter-controlled factors of fine-grained sediments in debris flow gullies are first summarized. Then, a relationship between stability inter-controlled factors of fine-grained sediments and outbreak probability of debris flow disasters is discussed.

- (1) The spatial distribution pattern of stability inter-controlled factors of fine-grained sediments in debris flow gullies is summarized.

We have summarized the spatial distribution characteristics of stability inter-controlled factors (grain size, permeability coefficient, and shear strength) of fine-grained sediment in the upstream, midstream, and downstream river: ① the average grain size of fine-grained sediments in the study area is 24.39 μm , belonging to silty loams. In space, it is characterized by relatively coarse grain size and poor sorting in the upstream and downstream river, and the grain size of sediments in the midstream river is relatively fine with good sorting; ② the average permeability coefficient of silty loams in the study area is 1.63 m/d, which can be classified as medium permeability. In space, it is relatively low in the upstream and downstream river and relatively high in the midstream river; ③ the average effective internal friction angle of silty loams in the study area is 20.24°, being a medium to low effective internal friction angle. In space, it is relatively low in the

upstream and downstream river and high in the midstream river. On the other hand, the average cohesion of silty loams in the study area is 22.99 kPa, belonging to the low cohesion level. In space, it is relatively high in the upstream and downstream river and low in the midstream river.

- (2) A relationship between stability inter-controlled factors of fine-grained sediments and outbreak probability of debris flow disasters has been discussed.

The outbreak of debris flow is the result of the comprehensive effects of sediment seepage field and stress field. Sediments with high stability (low permeability coefficient and high shear strength) are less prone to erosion, thus providing fewer material sources and forming a less dangerous debris flow disaster. On the contrary, sediments with low stability (high permeability coefficient and low shear strength) can provide more material sources to form a larger-scale and more dangerous debris flow disaster.

Author Contributions: Conceptualization, Q.W. and J.X.; methodology, Q.W., J.X., J.Y. and P.L.; validation, Q.W., J.X. and P.L.; formal analysis, Q.W. and J.X.; investigation, Q.W., J.X., P.L., W.X. and B.Y.; data curation, J.X., J.Y. and P.L.; writing—original draft preparation, Q.W., J.X. and J.Y.; writing—review and editing, Q.W.; visualization, W.X.; supervision, B.Y.; project administration, Q.W.; funding acquisition, Q.W. All authors have read and agreed to the published version of the manuscript.

Funding: This research was funded in part by the National Natural Science Foundation of China grant number 42071312, the Innovative Research Program of the International Research Center of Big Data for Sustainable Development Goals grant number CBAS2022IRP03, the National Key R&D Program grant number 2021YFB3900503, and the Second Tibetan Plateau Scientific Expedition and Research (STEP) grant number 2019QZKK0806.

Data Availability Statement: Data are contained within the article.

Conflicts of Interest: The authors declare no conflicts of interest.

References

1. Qu, Y. The research on the Dynamic Characteristics of Urgent Steep-channel Debris Flows in Meizoseismal Area. Ph.D. Thesis, Chengdu University of Technology, Chengdu, China, 2016. Available online: <https://kns.cnki.net/KCMS/detail/detail.aspx?dbname=CDFDLAST2020&filename=1019216954.nh> (accessed on 1 October 2023).
2. Li, Z. Study on the characteristics and outthrust of debris flow in steep gully in earthquake region. Master's Thesis, Chengdu University of Technology, Chengdu, China, 2019. Available online: <https://kns.cnki.net/KCMS/detail/detail.aspx?dbname=CMFD202001&filename=1019216296.nh> (accessed on 1 October 2023).
3. Qi, X.; Yu, B.; Zhu, Y. Experimental Study on the clastic deposition forming Debris Flow. *J. Jilin Univ.* **2014**, *44*, 1950–1959. [CrossRef]
4. Suo, W. Study on the Grain-size Distribution for Initiation and Catastrophe Mechanism of Slag-type Debris Flow. Master's Thesis, Chang'an University, Xi'an, China, 2019. Available online: <https://kns.cnki.net/KCMS/detail/detail.aspx?dbname=CMFD202001&filename=1019674844.nh> (accessed on 1 October 2023).
5. Fan, S. Solid Source Characteristics and Early Warning of Debris Flow in Zhouqu. Ph.D. Thesis, Lanzhou University, Lanzhou, China, 2018. Available online: <https://kns.cnki.net/KCMS/detail/detail.aspx?dbname=CDFDLAST2018&filename=1018829194.nh> (accessed on 1 October 2023).
6. Xiong, K. Study on Material Erosion Characteristics of Loose Accumulation on Slope after Jiuzhaigou Earthquake. Master's Thesis, Chengdu University of Technology, Chengdu, China, 2021. Available online: <https://kns.cnki.net/KCMS/detail/detail.aspx?dbname=CMFD202301&filename=1022671932.nh> (accessed on 1 October 2023).
7. Zhang, Z. Study On Erosion and Initiation Characteristics of Debris Flow Deposition Under the Influence of Rainfall and Over-dam Flow: A Case Study of Chutou Gully, Wenchuan, Sichuan. Master's Thesis, JiLin University, Changchun, China, 2022. Available online: <https://kns.cnki.net/KCMS/detail/detail.aspx?dbname=CMFD202202&filename=1022529781.nh> (accessed on 1 October 2023).
8. Gu, W. Study on Provenance Characteristics and Initiation Mechanism of Debris Flows in Meizoseismal Areas of Wenchuan Earthquake—Taking Study Areas, Gaochuan Village, Qingping Village and Yinxiu Town as Example. Master's Thesis, Chengdu University of Technology, Chengdu, China, 2015. Available online: <https://kns.cnki.net/KCMS/detail/detail.aspx?dbname=CMFD201601&filename=1015312750.nh> (accessed on 1 October 2023).
9. Yang, F.; Zhou, H.; Huo, M.; Cao, H.; Liang, Y.; Lin, K. Rainfall Induced Debris Flow Characteristics and Mechanisms of Plagues after the Outbreak of the Earthquake in Wenchuan. *China Rural. Water Hydropower* **2016**, *12*, 38–42+48.

10. Yu, Z.; Yuan, L.; Liu, J.; Liu, P.; Wu, H. Study on Distribution and Activity Characteristics of Giant Debris Flow in Wenchuan Earthquake Zone. *Subgrade Eng.* **2018**, *1*, 209–215. [[CrossRef](#)]
11. Tang, C.; Tie, Y. Reconnaissance and Analysis on the Rainstorm induced Debris Flow in Weijiagou Valley of Beichuan City after Wenchuan Earthquake. *J. Mt. Sci.* **2009**, *27*, 625–630.
12. Tie, Y.; Tang, C. Response Characteristics between Wenchuan Earthquake and the Rainfall Induced Debris Flow in Beichuan Country, Sichuan. *J. Catastrophology* **2011**, *26*, 73–75+81.
13. Luo, C.; Chen, T.; Fu, Q.; Chen, G.; Li, S. Analysis of Characteristics and Cause of Debris Flow in Yangjia Gully in Beichuan County. *J. Southwest Univ. Sci. Technol.* **2019**, *34*, 25–31.
14. Liu, S.; Kou, G.; Feng, J. Discussion on the geological environment of the causes on the debris flow in Beichuan County. *Technol. Innov. Appl.* **2018**, *01*, 177–179.
15. Legiman, M.K.A.; Mohamad, E.T.; Hasbollah, D.Z.A.; Suparmanto, E.K.; Rathinasamy, V. An overview of debris-flow mathematical modelling. *Phys. Chem. Earth* **2023**, *129*, 103301. [[CrossRef](#)]
16. Xia, X.; Jarsve, K.; Dijkstra, T.; Liang, Q.; Meng, X.; Chen, G. An integrated hydrodynamic model for runoff-generated debris flows with novel formulation of bed erosion and deposition. *Eng. Geol.* **2023**, *326*, 107310. [[CrossRef](#)]
17. Jiang, X.; Wörman, A.; Chen, X.; Zhu, Z.; Zou, Z.; Xiao, W.; Lia, P.; Liu, G.; Kang, D. Internal erosion of debris-flow deposits triggered by seepage. *Eng. Geol.* **2023**, *314*, 107015. [[CrossRef](#)]
18. Domènech, G.; Fan, X.; Scaringi, G.; van Asch, T.W.J.; Xu, Q.; Huang, R.; Hales, T.C. Modelling the role of material depletion, grain coarsening and revegetation in debris flow occurrences after the 2008 Wenchuan earthquake. *Eng. Geol.* **2019**, *250*, 34–44. [[CrossRef](#)]
19. Ma, C.; Hu, K.; Tian, M. Post-earthquake relationships of maximum runout amount and loose matter mass in debris flow gully. *J. Nat. Disasters* **2013**, *22*, 76–84. [[CrossRef](#)]
20. Wang, J. The Development Characteristics and Risk Assessment of High Debris Flow in Wenchuan Earthquake Area. Master's Thesis, Chengdu University of Technology, Chengdu, China, 2014. Available online: <https://kns.cnki.net/KCMS/detail/detail.aspx?dbname=CMFD201801&filename=1016227078.nh> (accessed on 1 October 2023).
21. Zhang, X. Study on Source Erosion, Movement Characteristics and Risk Assessment of Debris Flows—A Case Study of Debris Flows Along Du-Wen Highway. Master's Thesis, Chengdu University of Technology, Chengdu, China, 2015. Available online: <https://kns.cnki.net/KCMS/detail/detail.aspx?dbname=CMFD201601&filename=1015312745.nh> (accessed on 1 October 2023).
22. Wei, B.; Zhao, Q.; Han, G.; Zhang, H. Grey Correlation Method Based Hazard Assessment of Debris Flow in Quake-Hit Area—Taking Debris Flows in Beichuan as An Example. *J. Eng. Geol.* **2013**, *21*, 525–533.
23. Chang, M.; Dou, X.; Fan, X.; Yao, C. Critical Rainfall Patterns for Rainfall-induced Debris Flows in the Wenchuan Earthquake Area. *Geoscience* **2018**, *32*, 623–630. [[CrossRef](#)]
24. Chu, S. The Weathering Factor Study on the Formation of Gully—Type Debris Flow—Take Wenchuan Earthquake as an Example. Master's Thesis, Chengdu University of Technology, Chengdu, China, 2012. Available online: <https://kns.cnki.net/KCMS/detail/detail.aspx?dbname=CMFD201301&filename=1012500162.nh> (accessed on 1 October 2023).
25. Shi, S.; Tu, L.; Shen, W. Geological Characteristics and Dynamics Features of the Debris Flow in Yingtao Gully of Beichuan County, Sichuan Province. *Geol. Surv. Res.* **2014**, *37*, 34–38.
26. Wang, X. Hazard Assessment and Prevention of Wuxinggou Debris Flow in Beichuan County. Master's Thesis, Southwest University of Science and Technology, Mianyang, China, 2014. Available online: <https://kns.cnki.net/KCMS/detail/detail.aspx?dbname=CMFD201801&filename=1017720833.nh> (accessed on 1 October 2023).
27. Hu, S. The Prediction Explores of Secondary Geological Disaster Caused by 5.12 Earthquake in Beichuan County. Master's Thesis, Sichuan Normal University, Chengdu, China, 2015. Available online: <https://kns.cnki.net/KCMS/detail/detail.aspx?dbname=CMFD201601&filename=1015372910.nh> (accessed on 1 October 2023).
28. Mei, Y. 5.12 Earthquake in Beichuan County, Sichuan Province Area Debris Flow Hazard Assessment. Master's Thesis, Chengdu University of Technology, Chengdu, China, 2011. Available online: <https://kns.cnki.net/KCMS/detail/detail.aspx?dbname=CMFD2012&filename=1011235513.nh> (accessed on 1 October 2023).
29. Zhang, Q.; Pan, Q.; Chen, Y.; Luo, Z.; Shi, Z.; Zhou, Y. Characteristics of landslide-debris flow accumulation in mountainous areas. *Heliyon* **2019**, *5*, e02463. Available online: <http://creativecommons.org/licenses/by-nc-nd/4.0/> (accessed on 1 October 2023).
30. Hu, T. The Research on Formation Mechanism and Mitigation Measures of Large-Scale Debris Flow in the Wenchuan Earthquake Area. Ph.D. Thesis, Chengdu University of Technology, Chengdu, China, 2017. Available online: <https://kns.cnki.net/KCMS/detail/detail.aspx?dbname=CDFDLAST2020&filename=1019216142.nh> (accessed on 15 October 2023).
31. Zhang, S.; He, Y.; He, M. Source analysis and prevention plan determination of debris flow in Yangjiagou, Beichuan earthquake stricken area. *Sichuan J. Geol.* **2014**, *34*, 80–84.
32. Li, C.; Dong, T. Types and characteristics of geological disasters in Beichuan County. *J. Mianyang Teach. Coll.* **2017**, *36*, 93–97. [[CrossRef](#)]
33. Wang, Y. Hazard Assessment on Rainstorm Induced Debris Flows in Beichuan County of Wenchuan Earthquake Affected Area. Master's Thesis, Chengdu University of Technology, Chengdu, China, 2009. Available online: <https://kns.cnki.net/KCMS/detail/detail.aspx?dbname=CMFD2010&filename=2009221507.nh> (accessed on 15 October 2023).
34. Yuan, L.; Chen, X.; Wu, H.; Qiu, E. Study on Formation Mechanism of Debris Flow in Xijia Valley and the Engineering Measures for Control. *Subgrade Eng.* **2020**, *4*, 212–221. [[CrossRef](#)]

35. Hu, K.; You, Y.; Zhuang, J.; Chen, X. Characteristics and Countermeasures of Debris Flows in Beichuan's Meizoseismal Area. *Sci. Geogr. Sin.* **2010**, *30*, 566–570. [[CrossRef](#)]
36. Yu, Y.; Wei, L.; Chen, T. Characteristics of Debris flows and Control in Jiangjia Gully of Beichuan, Sichuan. *J. Geol. Hazards Environ. Preserv.* **2012**, *23*, 5–9.
37. Wu, Q.; Xu, L.; Zhou, K.; Liu, Z. Starting analysis of loose accumulation of gully-startup debris flow. *J. Nat. Disasters* **2015**, *24*, 89–96. [[CrossRef](#)]
38. Xie, M.; Wang, Y.; Zhang, H.; Zhao, Y.; Zhao, R. The Deposit Analysis of Water Dynamic Conditions to Form Debris Flow and to Set up Mathematical Model in Debris Flow Valley. *J. Beijing For. Univ.* **1993**, *15*, 1–11.
39. Xu, X.; Chen, J.; Shan, B. Study of Grain Distribution Characteristics of Solid Accumulation in Debris Flow. *Yangtze River* **2015**, *46*, 51–54. [[CrossRef](#)]
40. Wang, Q.; Xie, J.; Yang, J.; Liu, P.; Chang, D. A hyperspectral detection model for permeability coefficient of debris flow fine-grained sediments, Southwestern China. *Int. J. Digit. Earth* **2023**, *16*, 1589–1606. [[CrossRef](#)]
41. Wang, Q.; Xie, J.; Yang, J.; Liu, P.; Chang, D.; Xu, W. A Model between Cohesion and Its Inter-Controlled Factors of Fine-Grained Sediments in Beichuan Debris Flow, Sichuan Province, China. *Sustainability* **2022**, *14*, 12832. [[CrossRef](#)]
42. Wang, Q.; Xie, J.; Yang, J.; Liu, P.; Chang, D.; Xu, W. A Research on Cohesion Hyperspectral Detection Model of Fine-Grained Sediments in Beichuan Debris Flow, Sichuan Province, China. *Land* **2022**, *11*, 1609. [[CrossRef](#)]
43. Wang, Q.; Xie, J.; Yang, J.; Liu, P.; Chang, D.; Xu, W. Research on Permeability Coefficient of Fine Sediments in Debris-Flow Gullies, Southwestern China. *Soil Syst.* **2022**, *6*, 29. [[CrossRef](#)]
44. Yu, J. Study on Permeability Characteristic and Fine Particle Migration Law of Deposited Soil in Debris Flow Channel. Master's Thesis, Sichuan Normal University, Chengdu, China, 2020. Available online: <https://kns.cnki.net/KCMS/detail/detail.aspx?dbname=CMFD202101&filename=1020746689.nh> (accessed on 20 October 2023).
45. GB/T 50145-2007; Engineering Classification Standard for Soil. China Planning Press: Beijing, China, 2008.
46. Liu, Y. Research on Test Method for Permeability Coefficient of Cohesionless Coarse grained Soil in Hydraulic Engineering. *Shaanxi Water Resour.* **2020**, *12*, 211–213.
47. Sun, X.; Wang, D. Analysis of Soil Cohesion Values. *Liaoning Build. Mater.* **2010**, *3*, 39–42.

Disclaimer/Publisher's Note: The statements, opinions and data contained in all publications are solely those of the individual author(s) and contributor(s) and not of MDPI and/or the editor(s). MDPI and/or the editor(s) disclaim responsibility for any injury to people or property resulting from any ideas, methods, instructions or products referred to in the content.